

01  
**Simulation phenomenological model of laser-induced graphitized structures in diamond**

© D.N. Bukharov<sup>1</sup>, T.V. Kononenko<sup>2</sup>, A.O. Kucherik<sup>1</sup>

<sup>1</sup> Vladimir State University, Vladimir, Russia

<sup>2</sup> Prokhorov Institute of General Physics, Russian Academy of Sciences, Moscow, Russia

E-mail: buharovdn@gmail.com

Received April 18, 2024

Revised August 1, 2024

Accepted August 15, 2024

Models of the growth of laser-induced graphitized structures formed in diamond microcracks are proposed. The models are implemented within the framework of a cellular automaton with a Neumann neighborhood. It is shown that the proposed approximations do not contradict the results of experimental laser synthesis of graphitized structures and allow us to correctly describe the process of graphitization of the sample.

**Keywords:** diamond graphitization, diffusion approximation, cellular automaton, modeling.

DOI: 10.61011/TPL.2025.01.60130.19964

One of the unique features of diamond is its capacity to transform under high-temperature heating into another crystalline allotropic form (graphite) with radically different physical and chemical properties [1]. The process of thermally induced phase transformation is initiated at the surface and spreads gradually into the bulk of a diamond crystal. Pulsed laser irradiation [2–5] allows one to localize the transformation of diamond into graphite within a submicrometer region that may be moved within the crystal in any desired direction. The net result is that three-dimensional conductive microstructures of various shapes, which may serve as hardware components for ionizing radiation detectors [6], photonic crystals [7], integrated optical light guides [8], photoconductive antennas generating THz pulses [9], etc., are produced in the bulk of diamond.

Filamentary graphitized regions, which are normally formed by moving a laser caustic uniformly toward a laser beam [2–4], are one of the most commonly used types of laser-induced microstructures. Examples of such microstructures obtained under different laser irradiation conditions are presented in Fig. 1.

The emergence of characteristic lateral protrusions on microstructures is attributable to cracking of the diamond matrix under laser modification, which is confirmed by the results of scanning electron microscopy examination of the internal structure of the modified region [4]. The authors of [4] proposed the following explanation for the experimentally observed kinetics of growth of the graphitized region: numerous „activation centers“ are spread over the surface of resulting microcracks, and each center initiates the propagation of a thermally stimulated graphitization wave into the surrounding volume of diamond.

Graphitized structures may be characterized using a phenomenological model where the phenomenon is represented in a general form [10,11] within a simulation approach with a diffusion approximation, which, generally speaking,

provides a description of propagation processes of various nature [12,13]. The model is based on the solution of the diffusion equation in the discrete case implemented using the cellular automaton technique [14,15]. Although the observed processes are not, strictly speaking, diffusional, it is this type of processes that provide a fairly reliable description of the resulting structures.

The model figure was constructed within a rectangular computational domain with a uniform grid superimposed on it.

The key parameters of the model were motion velocity  $v_f$  of the laser radiation focus and probability  $s$  that a computational domain cell is occupied.

The initial condition for growth was the distribution of embryonic structures (activation centers) from which the graphitized region began to spread. The nature of the initial structure depended on parameter  $v_{cf}$  (critical motion velocity of the laser radiation focus) in the system. A continuous figure (straight line or fractal system of lines) was chosen as the initial structure when velocity  $v_f$  was below the critical  $v_{cf}$  level. When the velocity of the laser beam focus was above-critical, the initial figure was a distribution of points positioned far from each other. As the laser beam focus velocity increased beyond the critical value, the distance between these points increased in proportion to  $v_f/v_{cf}$ .

The procedure for constructing the model figure was a dynamic process of cell occupation originating at the initial structure, which was a model microcrack (Fig. 2, *a*). Computational domain cells adjacent to the current one were considered within the Neumann neighborhood (Fig. 2, *b*) [15]. The current cell became „occupied“ if there was at least one occupied cell in its Neumann neighborhood. In addition to this condition, the specified cell could become occupied with a given probability  $s$ ,

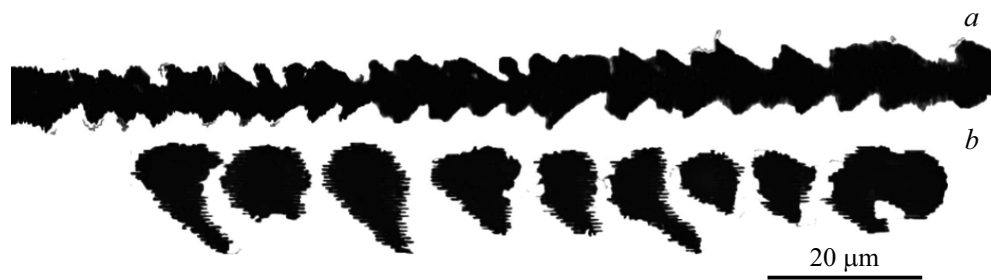


**Figure 1.** Optical photographic images of filamentary graphitized regions formed by 140 fs laser pulses at different caustic velocities  $v$ :  $a$  —  $30\ \mu\text{m/s}$  and  $b$  —  $100\ \mu\text{m/s}$  ( $P = 1.53\ \text{mW}$ ,  $f = 1\ \text{kHz}$ ).

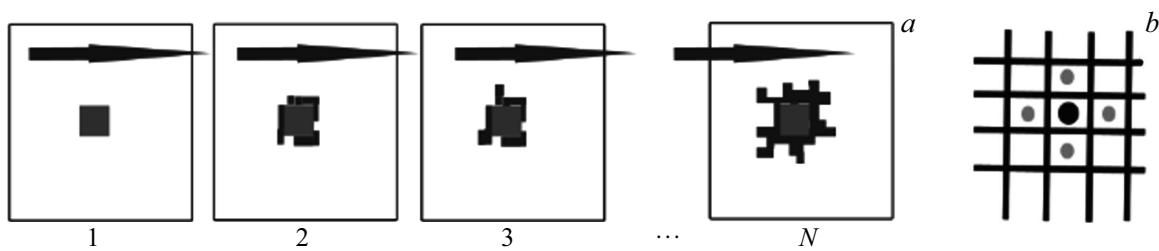


**Figure 2.** Model diagram:  $a$  — iterations of a 1- $N$  cellular automaton (growth proceeds from the initial structure in the center);  $b$  — Neumann neighborhood.

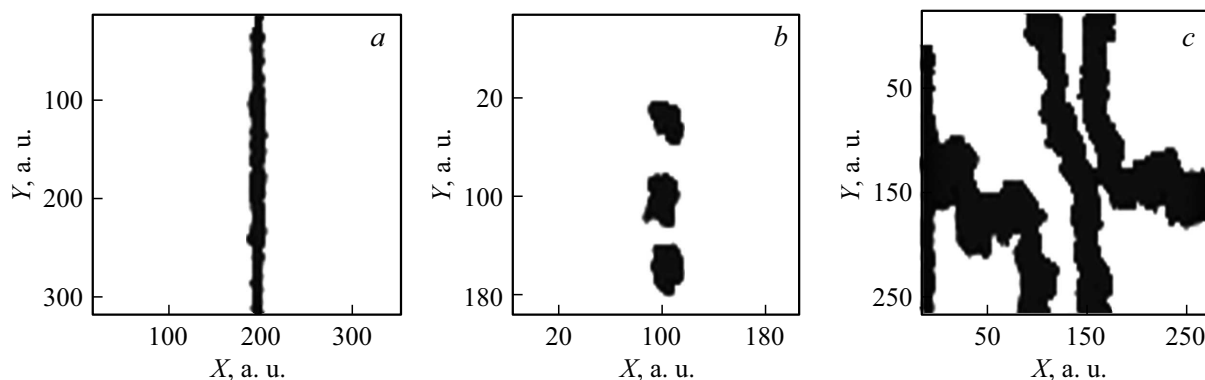


**Figure 3.** Results of simulation of the graphitized region.  $a$  —  $s = 0.075$ ,  $v_f < v_{cf}$ , and the initial structure is a straight line;  $b$  —  $s = 0.25$ ,  $v_f > v_{cf}$ , and the initial structure is a set of points;  $c$  —  $s = 0.5$ ,  $v_f < v_{cf}$ , and the initial structure is a system of fractal lines.

which may be considered proportional to temperature  $T$  to which it was heated.

The proposed model was implemented in MATLAB in relative units; the linear computational domain size was chosen to be the scaling factor. The input data for the software implementation of the model are the motion velocity of the laser radiation focus, its critical value, the temperature field for the computational domain, the computational domain size, and the number of iterations. Following a comparison of the entered velocity values, the initial distribution is generated from a pre-prepared image or via the generation of figures defined in the program (a straight line in the center of the computational domain or a system of points positioned at a certain distance from each other). Figure 3 presents the models of graphitized regions obtained under different initial conditions and different probabilities of a

cell being occupied within the same number of cellular automaton iterations ( $t = 800\ \text{a.u.}$ ) at  $v_{cf} = 34\ \mu\text{m/s}$  in an isothermal computational domain. Figure 3,  $a$  presents the continuous structure model generated from a straight line at  $v_f = 30\ \mu\text{m/s}$  and  $T = 4900^\circ\text{C}$ . Figure 3,  $b$  shows the graphitization region structure model with discontinuities at  $v_f = 100\ \mu\text{m/s}$  and  $T = 5000^\circ\text{C}$ . It is evident from Figs. 3,  $a$  and  $b$  that the width of model structures depends on parameter  $s$ : the width increases in proportion to it. Figure 3,  $c$  presents the graphitization region structure model generated from a system of fractal lines constructed using the DLA algorithm [16].

The fractal dimensions of images of the models and actual samples were compared in order to assess the accuracy of modeling. The fractal dimension was estimated using the box-counting method [17], which allowed us to compare

the distribution density of structural elements on a plane in the dimensionless form. The model shown in Fig. 3, *a* and the sample shown in Fig. 1, *a* were examined to evaluate the accuracy of the model. The calculated fractal dimensions of the actual sample and the model were 1.27 and 1.21, respectively. It is evident that the difference in fractal dimensions does not exceed 5%, suggesting that the model corresponds closely to the actual sample. This correspondence of fractal dimensions is likely to be translated into the correspondence of properties determined by topology (e.g., electrophysical or optical). In addition, the transition to absolute units made it possible to estimate the average width of the graphitized region. Specifically, with the lateral length of a computational domain cell being  $1\ \mu\text{m}$ , the average width of the model sample is  $10\ \mu\text{m}$ , which does not contradict the measurement results for the actual structure.

The proposed model allows one to evaluate the influence of control parameters of experimental synthesis on model samples. The model is related to these parameters via probability  $s$  as a relative temperature value. For example, the results of studies of the structure of graphitized regions obtained under pulsed laser irradiation indicate that one of the control parameters is the pulse duration: as it increases, the critical focal velocity also increases, which is accompanied by the emergence of discontinuities in the graphitization region. A tentative estimate of temperature as a function of pulse duration  $\tau$  is [18]

$$T(\tau) = \frac{2AP\sqrt{\alpha\tau}}{\pi^{3/2}kr_0} + T_s,$$

where  $A$  is the absorptance,  $P$  is the radiation power,  $\alpha$  is the temperature conductivity coefficient,  $k$  is the thermal conductivity coefficient, and  $T_s$  is the initial temperature. The relation between the model and control parameters may then be set as  $s(T) \sim T/S$ , where  $S$  is the area of the computational domain.

Thus, it can be concluded that the proposed model is applicable as a first approximation to the description of laser-induced graphitized structures in diamond.

The experimental study of formation of graphitized microstructures in diamond was conducted by T.V. Kononenko. The implementation of models and calculations of model structures were performed by D.N. Bukharov and A.O. Kucherik.

## Funding

This study was carried out under the state assignment of Vladimir State University „Development of Methods of Surface Laser Modification of Films Made of Synthetic Diamond and Wide-Bandgap Compositions Based on It for Control of the Optical and Electrophysical Properties of Structured Materials“ (FZUN-2023-0003).

## Conflict of interest

The authors declare that they have no conflict of interest.

## References

- [1] L. Muniraj, M. Ardrion, J.M. Fernández-Pradas, M. Duocastella, P. Serra, R.L. Reuben, D.P. Hand, *Sensors Actuators A*, **373**, 115442 (2024). DOI: 10.1016/j.sna.2024.115442
- [2] M. Shimizu, Y. Shimotsuma, M. Sakakura, T. Yuasa, H. Homma, Y. Minowa, K. Tanaka, K. Miura, K. Hirao, *Opt. Express*, **17**, 46 (2009). DOI: 10.1364/oe.17.000046
- [3] T.V. Kononenko, M.S. Komlenok, V.P. Pashinin, S.M. Pimenov, V.I. Konov, M. Neff, V. Romano, W. Lüthy, *Diamond Relat. Mater.*, **18**, 196 (2009). DOI: 10.1016/j.diamond.2008.07.014
- [4] K.K. Ashikkalieva, T.V. Kononenko, E.E. Ashkinazi, E.A. Obratsova, A.A. Mikhutkin, A.A. Timofeev, V.I. Konov, *Diamond Relat. Mater.*, **128**, 109243 (2022). DOI: 10.1016/j.diamond.2022.109243
- [5] B. Sun, P.S. Salter, M.J. Booth, *Appl. Phys. Lett.*, **105**, 231105 (2014). DOI: 10.1063/1.4902998
- [6] L. Anderlini, M. Bellini, V. Cindro, C. Corsi, K. Kanxheri, S. Lagomarsino, C. Lucarelli, A. Morozzi, G. Passaleva, D. Passeri, S. Sciortino, L. Servoli, M. Veltri, *Sensors*, **22**, 8722 (2022). DOI: 10.3390/s22228722
- [7] E. Granados, M. Martinez-Calderon, M. Gomez, A. Rodriguez, S.M. Olaizola, *Opt. Express*, **25**, 15330 (2017). DOI: 10.1364/OE.25.015330
- [8] A.N. Giakoumaki, G. Coccia, V. Bharadwaj, J.P. Hadden, A.J. Bennett, B. Sotillo, R. Yoshizaki, P. Olivero, O. Jedrkiewicz, R. Ramponi, S.M. Pietralunga, *Appl. Phys. Lett.*, **120**, 020502 (2022). DOI: 10.1063/5.0080348
- [9] S. Lepeshov, A. Krasnok, A. Krasnok, E. Rafailov, P. Belov, *Laser Photon. Rev.*, **11**, 160 (2017). DOI: 10.1002/lpor.201600199
- [10] N.I. Plusnin, *Phys. Solid State*, **61** (12), 2431 (2019). DOI: 10.1134/S1063783419120394
- [11] N.A. Agafonova, *Vestn. Ivanov. Gos. Energ. Univ.*, No. 4 (2007) (in Russian).
- [12] T. Trifonova, M. Arakelian, D. Bukharov, S. Abrakhin, S. Abrakhina, S. Arakelian, *Water*, **14**, 1405 (2022). DOI: 10.3390/w14091405
- [13] T.V. Ryzhova, D.N. Bukharov, S.M. Arakelyan, *Nauka Tekh.*, No. 4, 333 (2023) (in Russian). DOI: 10.21122/2227-1031-2023-22-4-333-34
- [14] S.K. Sarukhanyan, A.G. Maslovskaya, *Mat. Strukt. Model.*, No. 2 (70), 63 (2024) (in Russian). DOI: 10.24147/2222-8772.2024.2.63-79
- [15] E. Agyingi, L. Wakabayashi, T. Wiandt, S. Maggelakis, *Processes*, **6**, 207 (2018). DOI: 10.3390/pr6110207
- [16] J. Mroczka, M. Woźniak, F.R.A. Onofri, *Metrol. Meas. Syst.*, **19**, 459 (2012). DOI: 10.2478/v10178-012-0039-2
- [17] J. Yan, Y. Sun, S. Cai, X. Hu, *J. Appl. Anal. Comput.*, **6**, 1114 (2016). DOI: 10.11948/2016073
- [18] Y. Xu, R. Wang, S. Ma, L. Zhou, Y.R. Shen, C. Tian, *J. Appl. Phys.*, **123**, 025301 (2018). DOI: 10.1063/1.5008963

Translated by D.Safin